IL NUOVO CIMENTO **38 C** (2015) 76
DOI 10.1393/ncc/i2015-15076-3

COMMUNICATIONS: SIF Congress 2014

A laser-driven electron accelerator for radiobiology experiments

L. LABATE (*)

Istituto Nazionale di Ottica, Sezione di Pisa, Consiglio Nazionale delle Ricerche - Pisa, Italy

received 12 February 2015

Summary. — A novel concept laser-driven electron accelerator is described, whose operation regime and setup was optimized for radiobiology experiments. A brief account is given first of the motivations of our work, aimed at allowing irradiation campaigns of *in vitro* biological samples; the ultimate goal is to check the biological effectiveness of laser-driven electron beams against conventionally accelerated ones. A description of the electron source is then given; finally, the main results of the activity aimed at characterizing the source from a dosimetric point of view are presented.

PACS 52.38.Kd – Laser-plasma acceleration of electrons and ions.
PACS 87.50.cm – Dosimetry/exposure assessment.

1. – Introduction and motivations

The field of electron acceleration driven by ultrashort and ultraintense laser pulses has been experiencing an impressive development throughout the past decade, making it feasible the development of real laser-driven accelerators both in large scale facilities and small scale laboratories. Although the basic idea of using a high amplitude plasma wave, such as the one which can be excited in the wake of a travelling laser pulse, was suggested in 1979 [1], it took until the end of 90 s for the so-called Laser Wakefield Acceleration (LWFA) regime, the most effective of the different approaches proposed in that paper, to become accessible, namely after the introduction of the so-called Chirped Pulse Amplification technique [2], which allowed the amplification of ultrashort pulses up to ultrahigh power.

Roughly speaking, the LWFA process is basically activated by focusing an ultrashort ($\sim$ 100 fs duration) and powerful ($\gtrsim$ 10 TW) laser pulse onto a gas-jet target at an intensity $\gtrsim 10^{18}\,\mathrm{W/cm^2}$. With the laser systems currently available (based, in general,

(*) Also at Istituto Nazionale di Fisica Nucleare, Sezione di Pisa and Laboratori Nazionali di Frascati, Italy.

on Ti:sapphire gain media), delivering pulses with energy from a few hundreds mJ up to the few J level, this tipically involves the focusing of the beam down to spot sizes of the order of a few μm. Due to the field effect at such an ultrahigh intensity, the gas gets ionized over the first few laser cycles; furthermore, the ponderomotive force of the pulse (basically proportional to the gradient of the intensity) acts to push the free electrons out of the region of highest intensity, thus exciting a plasma wave if the pulse duration roughly matches half of the plasma wavelength at the given electron density. The resulting plasma wave then travels with a phase velocity, set by the laser pulse group velocity, close to c, and can thus accelerate, up to relativistic energies, electrons which get injected into it with the right phase (see [3] and references therein to gain further insight into the underlying physics). The interest in such a novel electron acceleration scheme mainly stems from the high accelerating gradients which can be established in a plasma, as compared to the ones achievable in a radiofrequency (RF) based acceleration stage. Indeed, in the latter case electric field amplitudes up to a few tens of MV/m can be obtained with present day technology RF cavities (see for instance [4]), to be compared with the tens or few hundreds of GV/m which can be established in a plasma wave (see for instance [5] for a review of the basic scaling laws). From a practical point of view, this results in a typical laser-driven "accelerator" stage, providing electron bunches in the 100 MeV–1 GeV energy range, having a centimeter scale. Experiments reported starting from 2004 [6-8] have been showing that quasi-monoenergetic electron bunches can be accelerated from the background plasma electron population up to hundreds MeV energy with an ever-increasing bunch quality. Very recently, a record energy in excess of 4 GeV, with 6% energy spread and 6 pC bunch charge has been reported [9].

Laser-driven accelerators are currently being studied for the design and construction of accelerators and colliders for high-energy physics experiments (see for instance [10]), as well as for the development of novel concept all-optical, tunable X/γ-ray secondary sources based upon the inverse Thomson/Compton scattering process [11-13] or external undulator [14]. Furthermore, electron accelerators based on the LWFA process and delivering electron bunches with energy in the range 10–100 MeV are deserving a growing attention for diverse applications, mainly due to their intrinsic reduced footprint when compared to conventional LINACs. This feature is of a particular importance in view of possible applications in medicine, and in particular for radiotherapy. As a matter of fact, over the past few years, laser-driven electron accelerators have been greatly evolving, in terms, for instance, of operation stability and reliability, so that their possible use for radiotherapy can now be foreseen within the next decade [15].

One of the radiotherapy protocols which is likely to be within the grasp of laser-driven accelerators in a very short time is the so-called Intra-Operatory Radiation Therapy (IORT) [17], due to its lower demanding requirements on the electron bunch features (such as, for instance, the electron spectrum, the bunch divergence and/or transverse emittance) as compared to other radiotherapy protocols. Indeed, the stable production of electron bunches with energy and divergence of interest for the IORT was demonstrated to be easily achievable using 10 TW-scale laser systems [16]. A typical IORT accelerator delivers electron bunches with energy up to around 10–12 MeV and employes a few tens of centimeters long RF cavity. Figure 1 shows a pictorial view of an operating theater where an IORT is administered using a conventional accelerator (left) and a fancy scheme of a corresponding situation using a laser-driven accelerator (right). From a practical point of view, this latter would exhibit a wealth of advantages in terms, for instance, of radioprotection requirements, versatility and flexibility. For instance, the usage of a laser-driven accelerator for IORT would allow a much smaller device to be introduced

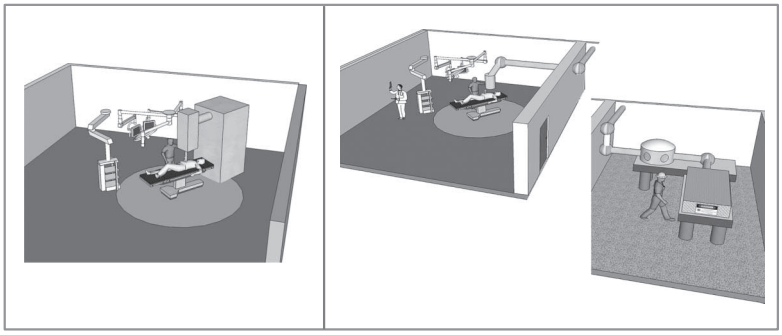

Fig. 1. – Pictorial view of an operating theater where an IORT radiotherapy is administered, in the case of use of a conventional, RF-based LINAC machine (left) and of a laser-driven accelerator (right). As is visible in the latter case, the laser beam, possibly serving different areas, can be easily transported, thus reducing the overall "accelerator" footprint into the operating theater and relaxing related issues such as radioprotection requirements, vacuum issues, and so on.

in the operating room, as the most bulky component, the laser system, may be placed and monitored outside, leaving only the "accelerator stage", a few centimeters in size, close to the patient. It is also worth to remind, at this stage, that electron bunches with energy up to a few 100 s MeV can be easily obtained while keeping the "accelerator stage" size within 10 cm; this allows, in principle, novel radiotherapy protocols to be developed, taking advantage of the higher energy available.

One of the most striking features of a laser-driven accelerator is the extremely short duration of the electron bunch, namely much smaller than in a conventional accelerator [18]. Indeed, while durations of a few up to a few tens of femtoseconds have been reported for the bunches on leaving the plasma, a bunch duration of a few picoseconds can be safely estimated/calculated at the position of the biological sample or patient (that is, after a few tens of centimeters propagation and possibly a vacuum-air interface); this value is still up to 5–6 orders of magnitude lower than the one of a typical LINAC used in radiotherapy. By taking into account the typical bunch charge in the two cases (which can be comparable or even higher), one can easily realize that a much higher instantaneous current, and thus instantaneous dose rate, is actually obtained, whose biological consequences have to be investigated in depth yet. On the other hand, the availability of such ultrashort electron bunches makes it possible to study the dynamics of the cell damage (and possibly, repair mechanisms) at early stages [19] and possibly opens up new fields of investigation in cell damage biology.

Further differences of a laser-driven accelerator as compared to a conventional one rely in the broader energy spectrum (when no advanced injection schemes are implemented, such as in the typical case of a tentatively "easy-to-use" accelerator for medicine) and a higher divergence. All of these issues demand for accurate studies related to both the dosimetric and the biological issues involved in the use of a laser-driven accelerator.

In this paper, we will be providing a brief outline of the multidisciplinary experimental activity which we're currently carrying out, aimed at a) establishing a stable and reliable laser-driven electron source in the 10–100 MeV energy range, targeting, as a first step, at the regime of interest for the IORT therapy; b) characterizing the source from a dosimetric point of view, possibly providing dosimetric figures as analogue as possible to the ones used in conventional radiotherapy dosimetry; c) carrying out cell irradiation experiments

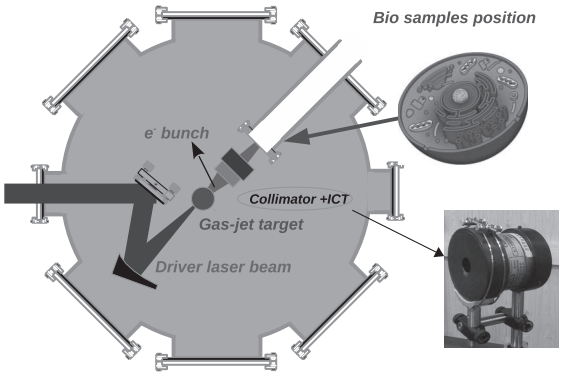

Fig. 2. – Schematic view of the experimental setup for radiobiology experiments. The gray area shows the vacuum chamber. In the inset, a picture of the ICT device, used to monitor from shot to shot the total electron bunch charge, is provided.

preliminarily aimed at assessing the biological response (at different cell biology levels) to ultrashort electron bunches. In particular, the paper is intended to focus on the first two issues and briefly list the range of biological measurements that are currently carried out in our laboratory. In the final section, we will draw some conclusions and give a brief discussion of the open issues and the future work.

2. – The LWFA electron source

An electron accelerator based on the LWFA process in a laser-produced plasma has been setup, over the past few years, at the Intense Laser Irradiation Laboratory of the National Institute of Optics of the CNR in Pisa, where a 10 TW Ti:Sa laser system is operating [20, 21]. The laser delivers up to 450 mJ on target and features an M^2 quality factor close to 1.5 and a nanosecond contrast of about 10^{10}. The LWFA regime selected for the radiobiology experiments was achieved by focusing the beam using an $f/4.5$ Off-Axis Parabolic mirror down to a spot size of around 10 μm FWHM; the intensity on target was about 8×10^{18} W/cm^2. The target was made up by a supersonic nitrogen (N_2) gas-jet, produced using a rectangular nozzle with size 4×1.2 mm (the laser propagation occurring along tha smallest size); the backing pressure was kept at 50 bar. A schematic layout of the setup inside the interaction chamber is provided in fig. 2. The laser-plasma interaction was monitored mainly using a shadowgraphy and a Thomson imaging diagnostic. Figure 3 shows on the left a Thomson image of the region of the plasma where the acceleration of the electrons occur. As is well known, in a Thomson scattering diagnostic the emitted light at the laser wavelength is roughly proportional, in a non-relativistic approximation, to the local electron density and the laser intensity. The image then allows the region where the laser pulse gets focused and propagates undepleted to be identified. Hence, this picture confirms what we said in the introduction, namely that the acceleration process occur on a very short ($\sim 100\,\mu$m) length. The electron production was seeked for and monitored using a LANEX scintillator screen imaged out by a commercial reflex camera and NaI scintillators coupled to photomultipliers (not shown in the figure). The electron spectrum was measured on a daily basis, at the beginning of each run, using a magnetic spectrometer, featuring a 1 T magnetic field and a 0.5 inch length and equipped with a LANEX screen imaged out by a commercial camera as

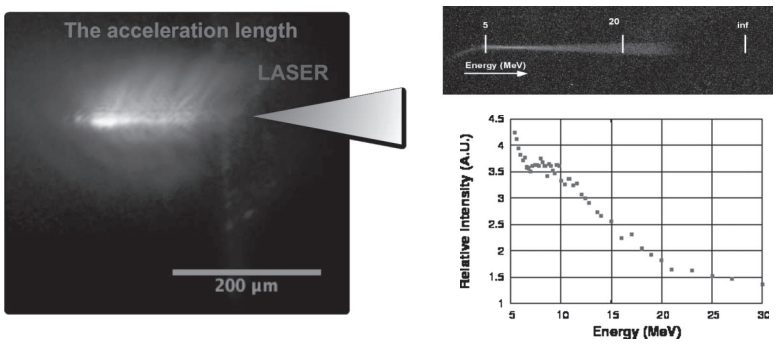

Fig. 3. – Left: time-integrated Thomson image of the plasma region, providing a visual estimate of the pulse propagation length. Right: top: raw image of the LANEX screen detector employed in the magnetic spectrometer; bottom: retrieved electron spectrum in the acceleration regime used for the radiobiology experiments.

a detector; its configuration allowed electrons with an energy greater than around 4 MeV to be detected. Figure 3 shows, on the right, a raw image of the LANEX scintillator screen and the corresponding retrieved spectrum. We selected such a spectrum (that is, the laser-plasma interaction regime providing such an electron spectrum) for our first radiobiology experiments, as electron energies in the range of a few up to around 10–12 MeV are routinely used in the IORT therapy nowadays [22]. In order to keep the cell samples to be irradiated as close as possible to the electron source, a tube was inserted on the chamber flange along the electron propagation direction, terminating with a vacuum-air interface for the electron beam made up by a 50 μm kapton layer. The electron beam production and total charge was measured on each shot using an Integrating Current Transformer (ICT) device, shown in the inset of fig. 2. Finally, in order to prevent unwanted high-energy electrons from spreading around in the vacuum chamber, a sort of collimator was used (visible in the figure), made up of a sandwich structure of different plastic and metallic layers with an overall length of around 10 cm.

3. – Dosimetric characterization of the source for radiobiology experiments

Although a careful control of the electron injection by advanced schemes allows the overall bunch quality to be improved (see [3] and references therein), laser-driven electron accelerators are, generally speaking, characterized by pretty different bunch parameters with respect to electrons accelerated by the LINACs currently in use for medical applications. Indeed, beside to the much smaller duration we discussed in the first section, laser-driven bunches feature a bunch divergence ranging from a few up to a few hundreds of mrad [23, 24] and a broad energy spectrum, with typical spectral width of a few tens up to one hundred percent. Moreover, a single electron bunch exhibits a total charge which can be one order of magnitude higher than the one from a LINAC used, for instance, in the IORT therapy. These circumstances requires a careful dosimetric characterization of a laser-driven source to be used for medical applications, and possibly the development of novel dosimetry techniques. To this purpose, we used type MD55-v2 or EBT3 GAF chromic films (GAF) packed in a stack and separated by RW3 solid water (see for instance [25]). Such a kind of measurement was performed both inside the vacuum chamber, at a distance of a few centimeters from the source, and after

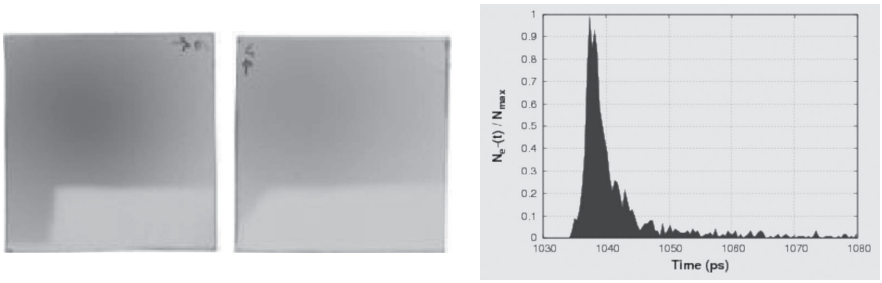

Fig. 4. – Left: raw scan of the first two layers of a stack of gafchromic films used to measure the electron flux and retrieve the available dose. Right: distribution of the arrival times of the electrons as simulated using a Monte Carlo code based on the GEANT4 library.

the vacuum-air electron interface, that is at the position of the biological samples. As an example, fig. 4, left, shows a scan of the first two gafchromic layers of a stack placed inside the vacuum chamber. The optical density of each film is proportional to the local delivered energy. In order to get quantitative dosimetric estimates from such a kind of measurements, we compared them against the results from a Monte Carlo simulation of the entire setup, based upon the GEANT4 library [26]. Further details of this procedure are reported in [27]. The Monte Carlo code also allows an estimate of the increase of the bunch duration upon arrival at the sample position to be obtained (this does not account, of course, for collective processes such as, for instance, the Coulomb repulsion). As an example, fig. 4, right, shows the distribution of the arrival times of the electrons at the sample position in the case of an initial exponential spectrum with around 6 MeV average energy. The width of the curve confirms that an electron bunch duration of a few picoseconds can be estimated for the electron bunch arriving on the biological samples.

Finally, dosimetric measurements allowed us to estimate an average dose of around 60 mGy to be delivered to the sample per laser shot in the acceleration regime selected for the radiobiology experiments. Since our accelerator can currently run at a repetition rate of about 0.5 Hz, doses of interest for the radiotherapy (~ 10 Gy) could be typically provided in few tens of seconds. As for the transverse profile of the electron beam, we found that a homogeneous, nearly flat-top beam profile with inhomogeneities of the order of 10% could be obtained, with a typical size at the sample position (that is, at around 20 cm from the source) of the order of 2 cm FWHM.

4. – Summary, discussion and open issues

We have briefly reported here on the development and characterization of a novel-concept laser-driven electron accelerator optimized for the irradiation of small (a few centimeters in transverse size) biological samples. Over the past few months, this novel accelerator has been being used to carry out experimental campaigns of irradiation of *in vitro* biological samples. In particular, such work was aimed at comparing the biological effectiveness of laser-driven bunches against conventionally accelerated ones at the same dose levels. To this purpose, different kinds of cell damages have been investigated by means of diverse biological tests, such as, for instance, the micronucleus assay, the measurement of the telomere shortening and the measurements of possible impairements in the cell membrane signalling. A full discussion of these issues is outside the scope of this paper and will be reported elsewhere.

From the point of view of the laser-plasma interaction, the work reported here mainly lied in looking for a stable and reliable LWFA regime providing an electron beam with relatively low energy ($\sim 10\,\mathrm{MeV}$) but with high charge. As a matter of fact, the dose retrieved by comparing the Monte Carlo simulations to the gafchromic stacks measurements allows a total electron charge greater than 1 nC for the electrons with energy $> 1\,\mathrm{MeV}$ to be estimated for each laser shot. This is actually a pretty remarkable value and was also confirmed by Particle-In-Cell simulations of the laser-plasma interaction. It is worth noting that such a high charge results from the relaxing of the requirement on the energy spread [28], as a trade-off exists between the two figures.

One of the major issues to be taken into account in order for a source to be employed for radiobiology experiments is the shot-to-shot stability, in terms of total bunch charge (affecting the dose delivered to the biological sample), electron energy spread and pointing stability. As for the first point, we estimated a fluctuation of the order of 10% RMS in the total charge over a few hundreds consecutive shots. While this is still not acceptable for a tentative clinical use of our source, it allows *in vitro* radiobiology experiments to be carried out, provided that the actual dose delivered on each sample is retrieved. In our radiobiology experiments, in order to have independent measurements, we employed both an Integrating Current Transformer device (shown in fig. 2) and stacks of gafchromic films placed both upstream and downstream the sample to be irradiated. Concerning the pointing stability, it can be claimed that fluctuations of the order of a few laser waist (at the focal position) could be obtained; these did not affect the biology experiments in our regime, since, as said above, a strongly diverging electron beam was actually produced and employed in order to have a large enough useful area at the sample position.

Finally, it should be pointed out that, as briefly mentioned above, the electron spectrum in our regime exhibits a pretty large width. Furthermore, a strong low-energy electron component was actually found, with energy $\lesssim 1\,\mathrm{MeV}$. The presence of such a component may actually hinder the studies aimed at assessing the biological effects on cell systems, due to the higher Relative Biological Effectiveness (RBE) of low-energy electrons as compared to higher energy ones. We are currently working on an energy selector, basically made up of a stack of permanent quadrupole magnets, to address this issue.

* * *

The author acknowledges collaboration with M. G. Andreassi, F. Baffigi, R. Bizzarri, A. Borghini, G. Bussolino, G. Candiano, C. Casarino, F. Di Martino, L. Fulgentini, P. Köster, F. Ghetti, M. C. Gilardi, A. Giulietti, D. Lamia, T. Levato, G. Russo, A. Sgarbossa, C. Traino and L. A. Gizzi. This work was carried out in the framework of the CNR High Field Photonics Unit (MD.P03.034). The author acknowledges financial support from the CNR funded Italian research Network ELI-Italy (Attoseconds), from the italian Ministry of Health through the project GR-2009-1608935 (D.I. AgeNaS) and from the PRIN project contract n. PRIN2012AY5LEL. The author also acknowledges contribution from the MIUR-FIRB project SPARX (Sorgente Pulsata Auto-Amplificata di Radiazione X).

REFERENCES

[1] Tajima T. and Dawson J. M., *Phys. Rev. Lett.*, **43** (1979) 267.
[2] Strickland D. and Mourou G., *Opt. Commun.*, **56** (1985) 219.
[3] Esarey E., Schroeder C. B. and Leemans W. P., *Rev. Mod. Phys.*, **81** (2009) 1229.

[4] Padamsee H., *Supercond. Sci. Technol.*, **14** (2001) R28.
[5] Lu W., Tzoufras M., Joshi C., Tsung F. S., Mori W. B., Vieira J., Fonseca R. A. and Silva L. O., *Phys. Rev. ST Accel. Beams*, **10** (2007) 061301.
[6] Faure J., Glinec Y., Pukhov A., Kiselev S., Gordienko S., Lefebvre E., Rousseau J.-P., Burgy F. and Malka V., *Nature*, **431** (2004) 541.
[7] Geddes C. G. R., Toth Cs., van Tilborg J., Esarey E., Schroeder C. B., Bruhwiler D., Nieter C., Cary J. and Leemans W. P., *Nature*, **431** (2004) 538.
[8] Mangles S. P. D., Murphy C. D., Najmudin Z., Thomas A. G. R., Collier J. L., Dangor A. E., Divall E. J., Foster P. S., Gallacher J. G., Hooker C. J., Jaroszinski D. A., Langley A. J., Mori W. B., Norreys P. A., Tsung F. S., Viskup R., Walton B. R. and Krushelnick K., *Nature*, **431** (2004) 535.
[9] Leemans W. P., Gonsalves A. J., Mao H.-S., Nakamura K., Benedetti C., Schroeder C. B., Tòth Cs., Daniels J., Mittelberger D. E., Bulanov S. S., Vay J.-L., Geddes C. G. R. and Esarey E., *Phys. Rev. Lett.*, **113** (2014) 245002.
[10] Leemans W. P., Duarte R., Esarey E., Fournier S., Geddes C. G. R., Lockhart D., Schroeder C. B., Toth C., Vay J. L. and Zimmermann S., *AIP Conf. Proc.*, **1299** (2010) 3.
[11] Powers N. D., Ghebregziabher I., Golovin G., Liu C., Chen S., Banerjee S., Zhang J. and Umstadter D. P., *Nature Photo.*, **8** (2014) 28.
[12] Sarri G., Corwan D. J., Schumaker W., Cole J. M., Di Piazza A., Ahmed H., Harvey C., Keitel C. H., Krushelnik K., Mangles S. P. D., Najmudin Z., Symes S., Thomas A. G. R., Yeung M., Zhao Z. and Zepf M., *Phys. Rev. Lett.*, **113** (2014) 224801.
[13] Gizzi L. A., Anania M. P., Gatti G., Giulietti D., Grittani G., Kando M., Krus M., Labate L., Levato T., Oishi Y. and Rossi F., *Nucl. Instrum. Methods Phys. Res. B*, **309** (2013) 202.
[14] Jaroszinski D. A., Bingham R., Brunetti E., Ersfeld B., Gallacher J., van der Geer J., Isaac R., Jamison S. P., Jones D., de Loos M., Lyachev A., Pavlov V., Reitsma A., Saveliev Y., Vieux G. and Wiggins S. M., *Philos. Trans. R. Soc. A*, **364** (2006) 689.
[15] Nicolai M., Sävert A., Renter M., Schnell M., Polz J., Jäckel O., Karsch L., Schürer M., Oppelt M., Pawelke J. and Kaluza M. C., *Appl. Phys. B*, **116** (2014) 643.
[16] Giulietti A., Bourgeois A., Ceccotti T., Davoine S., Dobosz S., D'Oliveira P., Galimberti M., Galy J., Gamucci A., Giulietti D., Gizzi L. A., Hamilton D. J., Lefebvre E., Labate L., Marquès J. R., Monot P., Popescu H., Rèau F., Sarri G., Tomassini P. and Martin P., *Phys. Rev. Lett.*, **101** (2008) 105002.
[17] Beddar A. S., Biggs P. J., Chang S., Ezzell G. A., Faddegon B. A., Hensley F. W. and Mills M. D., *Med. Phys.*, **33** (2006) 1476.
[18] van Tilborg J., Schroeder C. B., Filip C. V., Tóth Cs., Geddes C. G. R., Fubiani G., Huber R., Kaindl R. A., Esarey E. and Leemans W. P., *Phys. Rev. Lett.*, **96** (2006) 014801.
[19] Malka V., Faure J. and Gauduel Y. A., *Mutation Res.*, **704** (2010) 142.
[20] Bussolino G. C., Faenov A., Giulietti A., Giulietti D., Köster P., Labate L., Levato T., Pikuz T. and Gizzi L. A., *J. Phys. D: Appl. Phys.*, **46** (2013) 245501.
[21] Labate L., Andreassi M. G., Baffigi F., Basta G., Bizzarri R., Borghini A., Candiano G. C., Casarino C., Cresci M., Di Martino F., Fulgentini L., Ghetti F., Gilardi M. C., Giulietti A., Köster O., Lenci F., Levato T., Oishi Y., Russo G., Sgarbossa A., Traino C. and Gizzi L. A., *Proc. SPIE*, **8779** (2013) 87790O-1.
[22] Righi S., Karaj E., Felici G. and Di Martino F., *J. Appl. Clin. Med. Phys.*, **14** (2013) 6.
[23] Brunetti E., Shanks R. P., Manahan G. G., Islam M. R., Ersfeld B., Anania M. P., Cipiccia S., Isaac R. C., Raj G., Vieux G., Welsh G. H., Wiggins S. M. and Jaroszinski D. A., *Phys. Rev. Lett.*, **105** (2010) 215007.

[24] Grittani G., Anania M. P., Gatti G., Giulietti D., Kando M., Krus M., Labate L., Levato T., Londrillo P., Rossi F. and Gizzi L. A., *Nucl. Instrum. Methods Phys. Res. A*, **740** (2014) 257.
[25] Galimberti M., Giulietti A., Giulietti D. and Gizzi L. A., *Rev. Sci. Instrum.*, **76** (2005) 053303.
[26] Agostinelli S. *et al.*, *Nucl. Instrum. Methods Phys. Res. A*, **506** (2003) 250.
[27] Lamia D. *et al.*, submitted to *Nucl. Instrum. Methods Phys. Res. A*.
[28] Reitsma A. J. W., Cairns R. A., Bingham R. and Jaroszinski D. A., *Phys. Rev. Lett.*, **94** (2005) 085004.